Evaluation of Hybrid Dedicated/Ambient EH for AF Relaying

Yulin Zhou, Erik Kampert, Yunfei Chen, Matthew D. Higgins

***Abstract*—In this letter, three hybrid simultaneous wireless information and power transfer (SWIPT)/ambient energy harvesting (EH) structures are analyzed for a relay node harvesting power from both a source node and the ambient environment. The EH structures are based on an ambient energy channel estimation power splitting scheme (ACEPS), an ambient energy data transmission power splitting scheme (ADTPS), and an ambient energy combination power splitting scheme (ACPS). Closed-form expressions of the achievable rates are derived. Numerical results are demonstrated to obtain the best proportion from these different schemes.**

***Index Terms*—AF relaying, Ambient RF, Energy Harvesting**

I. Introduction

Radio frequency (RF) energy harvesting has been proposed as a solution to powering relays [1]. The information signal received by the relay is forwarded to the destination using the energy harvested from the source [2], or ambient RFEH [3]. The ambient RF energy has a low power density between $0.2\ \mathrm{nW/cm^2}$ [4] and $\sim\ 1\ \mathrm{W/cm^2}$ [3], but it currently is steadily increasing due to the boom of wireless communication and broadcasting infrastructures, such as analogue/digital TV, AM/FM radio, WiFi networks, and 4G/5G cellular networks [5]. Historically, the ambient RF power density is more powerful in urban areas and in the proximity of the power sources (e.g., cell base station towers) [3]. This has inspired us to develop structures that combine EH from a source with ambient RFEH.

Current thinking in the community is dominated by either considering the systems with relay RF ambient EH and channel estimation without data transmission [6], or relay merely harvested energy from the source without examining the ambient energy [7]. In [8], the average output DC power in ambient RF energy harvesting has been analyzed through the effects of antenna directivity and antenna port number. To improve the use of the energy harvested from the environment, authors in [9] proposed an opportunistic routing which can effectively reduce the delay and improve the transmission success rate in energy-harvesting wireless sensor networks with dynamic transmission power. In [10], the authors optimized the power allocation as a non-cooperative game with SWIPT in small cell networks. More studies of EH relaying in vehicular networks using distributed beamforming(DB) are intended to learn the reliability and capacity of EH relaying. A DB-based EH relaying scheme was proposed for vehicular networks in [11]. Therefore, in this letter both are considered concurrently. None of them has considered both ambient RFEH and source EH.

Different types of wireless energy sources coexist in the ambient. Also, most systems suffer from interference between users, and the interference can be harvested as energy. For the senor networks or cellular networks, the users are moving all the time. Thus, wireless energy harvesting can significantly elevate the energy performance and extend lifetime. Motivated by these findings, this letter takes additional RF ambient energy into account, thus increasing the amount of energy harvested by the relay node. The information sent from relay to destination uses the energy harvested from the source and ambient environment without the relay's own power. Since ambient energy is out-of-band, the performance of the communication link is independent of its power level, and its system model value can be set at will. Based on the schemes designed in [12], three hybrid structures are designed based on a channel estimation power splitting scheme (CEPS), a data transmission power splitting scheme (DTPS) and a combination power splitting scheme (CPS). The cumulative density functions (CDFs) are derived. Then, the expressions for the achievable rate (AR) are developed. The system performance is investigated in terms of AR for different channel estimation rates and power splitting ratios.

II. System Models

In this section, the three system models Channel estimation power splitting scheme with ambient energy (ACEPS), Data transmission power splitting scheme with ambient energy (ADTPS), and Combination power splitting scheme with ambient energy (ACPS) are explained in details. The system structures examined in this letter are shown in Fig.1. Under the AF relaying frame, there is one source (S), one relay (R) and one destination (D). Each system works in half-duplex mode with a single antenna. Two hops are included in the transmission: SR and RD. The distances between source and relay, relay and destination, and source and destination are denoted as d_{sr}, d_{rd}, d_{sd}, respectively. The fading gains for

This work was supported in part by the WMG centre High Value Manufacturing Catapult, University of Warwick, Coventry, U.K.

Y. Zhou is with the Ningbo Research Institute, Zhejiang University, Ningbo 315100, China. (e-mail: zhou.yulin@outlook.com.)

E. Kampert, and M. D. Higgins are with WMG, University of Warwick, Coventry CV4 7AL, U.K. (e-mail: zhou.yulin@outlook.com; e.kampert@warwick.ac.uk; m.higgins@warwick.ac.uk.)

Y. Chen is with the School of Engineering, University of Warwick, Coventry CV4 7AL, U.K. (e-mail: yunfei.chen@warwick.ac.uk).

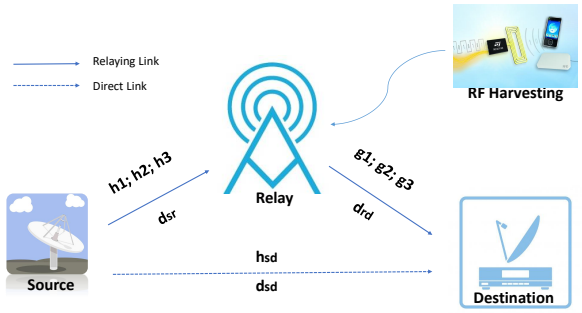

Fig. 1. AF relaying network.

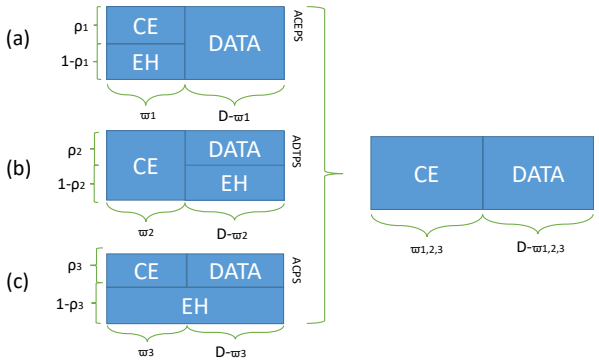

Fig. 2. (a) Channel estimation power splitting scheme with ambient energy (ACEPS); (b) Data transmission power splitting scheme with ambient energy (ADTPS); (c) Combination power splitting scheme with ambient energy (ACPS).

different structures in the channel between the source and the relay, h_1, h_2 and h_3, and between the relay and the destination, g_1, g_2 and g_3, are complex Gaussian with mean zero and variance $2\theta^2$. Fig. 2(a), 2(b) and 2(c) display the ACEPS, ADTPS and ADTPS scheme with power splitting ratio ρ_1, ρ_2, ρ_3 and ϖ_1, ϖ_2, ϖ_3 pilots for the channel estimation, respectively.

In the first hop, the received pilot signals for EH are [12]

$$y_r(i_m) = \sqrt{\frac{(1-\rho_m)P_{s_m}}{d_{sr}{}^e}}h_m x[i_m] + n_{m_1}(i_m) \quad (1)$$

where $m = 1, 2, 3$ represent the ACEPS; ADTPS and ACPS scheme, respectively; $i_1 = 1, 2, \ldots, \varpi_1; i_2 = 1, 2, \ldots, D - \varpi_2; i_3 = 1, 2, \ldots, D$; P_{s_m} is the transmission power of the source, e is the path loss exponent, $x[i_m]$ is the transmitted pilot symbol with unit power $E\{|\, x[i_m]\,|^2\} = 1$, and $n_{m_1}(i_m)$ is the complex additive white Gaussian noise (AWGN) with zero-mean and noise power N_{m_1}.

Thus, the harvested powers at the relays for use in transmission are

$$\hat{P_{tp_m}} = \begin{cases} \frac{\eta P_{s1}}{d_{sr}{}^e D}|\hat{h_1}|^2(1-\rho_1)\varpi_1 + \frac{\eta P_{ap1}}{D} & (a) \\ \frac{\eta P_{s2}}{d_{sr}{}^e D}|\hat{h_2}|^2(1-\rho_2)(D-\varpi_2) + \frac{\eta P_{ap2}}{D} & (b) \\ \frac{\eta P_{s3}}{d_{sr}{}^e D}|\hat{h_3}|^2(1-\rho_3)D + \frac{\eta P_{ap3}}{D} & (c) \end{cases} \quad (2)$$

where $\hat{h_m} = h_m + \varepsilon_{m_1}$ is the estimate of h_m, and $\varepsilon_{11,31} = \frac{\Sigma_{j_{1,3}=1}^{\varpi_{1,3}} n_{11,31}[j_{1,3}]}{\varpi_{1,3}\sqrt{\frac{P_{s1,s3}}{d_{sr}{}^e}}}; \varepsilon_{12} = \frac{\Sigma_{j_2=1}^{\varpi_2} n_{21}[j_2]}{\varpi_2\sqrt{\frac{\rho_2 P_{s2}}{d_{sr}{}^e}}}$ are the estimation errors. P_{ap_m} is the out-of-band ambient RF energy harvested by the relay node, and η is the conversion efficiency of the energy harvester.

For the second hop, the received data signals at the destination are written as [12]

$$y_d[k_m] = \sqrt{\frac{\hat{P_{tp_m}}}{d_{rd}{}^e}}g_m\hat{a}_{m_{var}}[\sqrt{\frac{z_m P_{s_m}}{d_{sr}{}^e}}h_m x[k_m] + n_{m_1}(k_m)] + n_{m_2}[k_m] \quad (3)$$

where $k_m = \varpi_m + 1, \ldots\ldots, D$, where P_{r_m} is the power preserved at m_{th} relay, $n_{m_2}[j_m]$ is AWGN with zero-mean and noise power N_{m_2}, $z_1 = 1; z_2 = \rho_2; z_3 = \rho_3$, d_{rd} is the distance between relay and destination, and the amplification factor can be written as $\hat{a}^2_{m_{var}} = \frac{1}{\frac{P_{s_m}|\hat{h_m}|^2}{d_{sr}{}^e} + N_{m_1}}$. The channel gain in the second hop is estimated as $\hat{g_m} = \sqrt{\frac{P_{r_m}}{\hat{P_{r_m}}}}g_m + \varepsilon_{m_2}$, where P_{r_m} is the power preserved at the m_{th} relay, and $\varepsilon_{m_2} = \frac{\Sigma_{j_m=1}^{\varpi_m} n_{m_2}[j_m]}{\varpi_m \hat{a}_{m_{var}}\sqrt{\frac{P_{r_m}}{d_{rd}{}^e}}}$ are the estimation errors. At the destination, the received data symbols at the destination in the direct link can be expressed as

$$y_d[k_m] = \sqrt{\frac{P_{s_m}}{d_{sd}{}^e}}h_{sd}x[k_m] + n_{sd}[k_m] \quad (4)$$

where d_{sd} is the distance between source and destination, and $n_{sd}[k_m]$ is the complex AWGN with mean zero and noise power N_{sd}.

III. End-to-end SNR

Using the end-to-end SNRs of the ACEPS, ADTPS and ACPS structures can be written as

$$\gamma_{end_m} = \frac{E[|\sqrt{\frac{\hat{P_{r_m}}}{d_{rd}{}^e}}\hat{g_m}\hat{a}_{m_{var}}\sqrt{\frac{z_m P_{s_m}}{d_{sr}{}^e}}\hat{h_m}x[j_{m_1}]|^2]}{Um} \quad (5)$$

where $Um = E[|\sqrt{\frac{\hat{P_{r_m}}}{d_{rd}{}^e}}\hat{g_m}\hat{a}_{m_{var}}\sqrt{\frac{z_m P_{s_m}}{d_{sr}{}^e}}\varepsilon_{m_1}x[j_{m_1}]|^2] + E[|\sqrt{\frac{\hat{P_{r_m}}}{d_{rd}{}^e}}\hat{g_m}\hat{a}_{m_{var}}n_{m_1}[j_{m_2}]|^2] + E[|\sqrt{\frac{\hat{P_{r_m}}}{d_{rd}{}^e}}\varepsilon_{m_2}\hat{a}_{m_{var}}n_{m_1}[i_m]|^2] + E[|n_{m_2}[j_{m_2}]|^2] + E[|\sqrt{\frac{\hat{P_{r_m}}}{d_{rd}{}^e}}\sqrt{\frac{z_m P_{s_m}}{d_{sr}{}^e}}\hat{h_m}\hat{a}_{m_{var}}\varepsilon_{m_2}x[j_{m_1}]|^2] + E[|\sqrt{\frac{\hat{P_{r_m}}}{d_{rd}{}^e}}\sqrt{\frac{z_m P_{s_m}}{d_{sr}{}^e}}\hat{a}_{m_{var}}\varepsilon_{m_1}\varepsilon_{m_2}x[j_{m_1}]|^2] + E[|n_{m_2}[j_{m_2}]|^2]$ and $z_1 = \rho_p; z_2 = \rho_d; z_3 = \rho_c$, respectively.

Similarly, the instantaneous direct link SNR in (4) is

$$\gamma_{sd} = \frac{\frac{P_{s1}}{d_{sd}{}^e}|h_{sd}|^2}{\frac{P_{s1}}{d_{sd}{}^e}Var(\varepsilon_{sd}) + N_{sd}} = \frac{\frac{P_{s1}}{d_{sd}{}^e}|h_{sd}|^2}{\frac{N_{sd}}{D} + N_{sd}}. \quad (6)$$

IV. Achievable rate analysis

A. ACEPS

$\hat{h_1}$ and $\hat{g_1}$ are needed; $|\hat{h_1}|^2$ is an exponential random variable with scale parameter $\lambda_{11} = \frac{1}{2\theta^2 + \frac{{d_{sr}}^e N_{11}}{\varpi_1 \rho_1 P_{s1}}}$, and $|\hat{g_1}|^2$ is an exponential variable with a scale parameter approximated as

$$\lambda_{12} = \frac{1}{r1} \tag{7}$$

where

$r1 = \frac{4\theta^4}{2\theta^2 + \frac{|N_{11} {d_{sr}}^e|}{\varpi_1 \rho_1 P_{s1}}} + \frac{N_{12}|DT{d_{rd}}^e|\lambda_{11}}{\varpi_1}[\frac{\frac{P_{s1}}{{d_{sr}}^e}}{\eta \frac{P_{s1}}{{d_{sr}}^e}|1-\rho_1|\varpi_1 T \lambda_{11}}$
$+ \frac{N_{11}\eta \frac{P_{s1}}{{d_{sr}}^e}|1-\rho_1|\varpi_1 T - \frac{P_{s1}}{{d_{sr}}^e}P_{ap1}}{(\eta \frac{P_{s1}}{{d_{sr}}^e}|1-\rho_1|\varpi_1 T)^2}(-e^{\lambda_{11}\frac{\eta \frac{P_{s1}}{{d_{sr}}^e}|1-\rho_1|\varpi_1 T P_{ap1}}{(\eta \frac{P_{s1}}{{d_{sr}}^e}|1-\rho_1|\varpi_1 T)^2}}$
$Ei(-\lambda_{11}\frac{\eta \frac{P_{s1}}{{d_{sr}}^e}|1-\rho_1|\varpi_1 T P_{ap1}}{(\eta \frac{P_{s1}}{{d_{sr}}^e}|1-\rho_1|\varpi_1 T)^2}))]$.

By using the above expressions, the CDF of γ_{end_1} is

$$\begin{aligned}
&P_{op_1}\{\gamma_{end_1} < \gamma_{1_{th}}\} = F_{\gamma_{end_1}}(\gamma_{1_{th}}) \\
&= \int_0^{\frac{\gamma_{1th}N_{11}}{m_1\rho_p P_{s1}} + \frac{\gamma_{1th}N_{11}}{P_{s1}}} f_{|\hat{h_1}|^2}(|\hat{h_1}|^2)dy + \\
&\int_{P_{s1}|\hat{h_1}|^2 - \frac{\gamma_{1th}N_{11}}{m_1\rho_p} - \gamma_{1th}N_{11}}^{\infty} F_{|\hat{g_1}|^2}[\frac{b_1}{d_1}\frac{(a_1+2b_1c_1)d_1 - b_1(d_1c_1+g_1)}{d_1^2 t + d_1(d_1c_1+g_1)} \\
&+ \frac{\frac{ac+b_1c_1^2}{d_1c_1+g_1}}{\frac{d_1}{d_1c_1+g_1}t^2+t}]f_{|\hat{h_1}|^2}(\frac{t}{P_{s1}} + \frac{\gamma_{1th}N_{11}}{m_1\rho_p P_{s1}} + \frac{\gamma_{1th}N_{11}}{P_{s1}})d_1 t
\end{aligned} \tag{8}$$

The integral is too complicated to solve. We use curve fitting of $e^{-\frac{1}{t+\frac{d_1c_1+g_1}{d_1}}} => [(0.17{m_1}^{-0.83} - 0.51)x^{0.15{m_1}^{-0.86}-0.6}e^{(-0.00516{m_1}^{-0.66}-0.041)x} + 0.9881]$ and $e^{-\frac{1}{\frac{d_1}{d_1c_1+g_1}t^2+t}} => [(-0.178{m_1}^{-0.7289} - 0.27)x^{0.33{m_1}^{-0.97}-1.68}e^{(-0.00518{m_1}^{-0.838}+0.0296)x} + 1.002]$ to simplify it. After curve fitting, the outage probability can be derived as

$$\begin{aligned}
&P_{op1} = 1 - \frac{e^{-\frac{\lambda_{12}m_1\gamma_{1th}N_{12}\rho_1 DT{d_{rd}}^e}{\rho_1{m_1}^2\eta(1-\rho_1)m_1 T}}}{\frac{P_{s1}}{{d_{sr}}^e}\left(2\theta^2 + |\frac{N_{11}}{m_1\rho_1\frac{P_{s1}}{{d_{sr}}^e}}|\right)} e^{-\frac{\gamma_{1th}N_{11}+\gamma_{1th}N_{11}m_1\rho_1}{2\theta^2 m_1\rho_1\frac{P_{s1}}{{d_{sr}}^e}+N_{11}}} \\
&(0.17{m_1}^{-0.83} - 0.51)^{\alpha_1} \times (-0.178{m_1}^{-0.729} - 0.27)^{\alpha_2} \\
&\frac{\Gamma([(0.15{m_1}^{-0.86} - 0.6)\alpha_1 + (0.33{m_1}^{-0.97} - 1.68)\alpha_2] + 1)}{{z_1}^{[(0.15{m_1}^{-0.86}-0.6)\alpha_1 + (0.33{m_1}^{-0.97}-1.68)\alpha_2]+1}}
\end{aligned} \tag{9}$$

where $a_1 = \gamma_{1th}N_{12}N_{11}DT + \varpi_1\rho_1\gamma_{1th}N_{12}N_{11}DT + \gamma_{1th}\varpi_1^2\rho_1 N_{12}DT; b_1 = \varpi_1\gamma_{1th}N_{12}\rho_1 DT; c_1 = \frac{\gamma_{1th}N_{11}}{\varpi_1\rho_1} + \gamma_{1th}N_{11}; d_1 = \rho_1{\varpi_1}^3\eta(1-\rho_1)T; g_1 = \eta\rho_1{\varpi_1}^2 P_{ap1}$, where $\alpha_1 = \frac{\lambda_{12}(a_1+2b_1c_1)}{d_1} - \frac{\lambda_{12}b_1(d_1c_1+g_1)}{d_1^2}$, $\alpha_2 = \frac{\lambda_{12}(ac+b_1c_1^2)}{d_1c_1+g_1}$ and $z_1 = [(0.15{m_1}^{-0.86} - 0.6)\alpha_1 + (0.33{m_1}^{-0.97} - 1.68)\alpha_2] + 1$, $z_1 = [(0.00516{m_1}^{-0.66} + 0.041)\alpha_1 + (0.00518{m_1}^{-0.838} - 0.0296)\alpha_2 + \frac{m_1\rho_1}{2\theta^2 m_1\rho_1 P_{s1} + N_{11}}]$.

B. ADTPS

$\hat{h_2}$ is a complex exponential variable with scale parameter $\lambda_{21} = \frac{1}{2\theta^2 + |\frac{{d_{sr}}^e N_{21}}{\varpi_2 P_{s2}}|}$ and $\hat{g_2}$ has a scale parameter appoximated as

$$\lambda_{22} = \frac{1}{r2} \tag{10}$$

where

$r2 = \frac{4\theta^4}{2\theta^2 + \frac{|N_{21}|{d_{sr}}^e}{\varpi_2 P_{s2}}} + \frac{N_{22}|DT{d_{rd}}^e|\lambda_{21}}{\varpi_2}[\frac{\frac{P_{s2}}{{d_{sr}}^e}}{\eta\frac{P_{s2}}{{d_{sr}}^e}|1-\rho_2|(D-\varpi_2)T\lambda_{21}} +$
$\frac{N_{21}\eta\frac{P_{s2}}{{d_{sr}}^e}|1-\rho_2|(D-\varpi_2)T - \frac{P_{s2}}{{d_{sr}}^e}P_{ap2}}{(\eta\frac{P_{s2}}{{d_{sr}}^e}|1-\rho_2|(D-\varpi_2)T)^2}(-e^{\frac{\lambda_{21}\eta\frac{P_{s2}}{{d_{sr}}^e}|1-\rho_2|(D-\varpi_2)TP_{ap2}}{(\eta\frac{P_{s2}}{{d_{sr}}^e}|1-\rho_2|(D-\varpi_2)T)^2}}$
$(-\frac{\lambda_{21}\eta\frac{P_{s2}}{{d_{sr}}^e}|1-\rho_2|(D-\varpi_2)TP_{ap2}}{(\eta\frac{P_{s2}}{{d_{sr}}^e}|1-\rho_2|(D-\varpi_2)T)^2}))]$.

Thus,

$$\begin{aligned}
&P_{op_2}\{\gamma_{end_2} < \gamma_{2th}\} = F_{\gamma_{end_2}}(\gamma_{2th}) \\
&= \int_0^{\frac{\gamma_{2th}N_{21}}{m_2P_{s2}} + \frac{\gamma_{2th}N_{21}}{\rho_d P_{s2}}} f_{|\hat{h_2}|^2}(y)dy = F_{|\hat{h_2}|^2}(y)dy \\
&\int_{\frac{\gamma_{2th}N_{21}}{m_2\rho_d P_{s2}} + \frac{\gamma_{2th}N_{21}}{P_{s2}\rho_d}}^{\infty} F_{|\hat{g_2}|^2}[\frac{b_2}{d_2} + \frac{(\frac{a_2}{\rho_d} + 2b_2c_2)\frac{d_2}{\rho_d} - \frac{b_2}{\rho_d}(d_2c_2+g_2)}{\frac{d_2^2}{{\rho_d}^2}t + \frac{d_2}{\rho_d}(d_2c_2+g_2)} \\
&+ \frac{\frac{a_2c_2+b_2c_2^2\rho_d}{d_2c_2+g_2}}{\frac{d_2}{(d_2c_2+g_2)\rho_d}t^2+t}]f_{|\hat{h_2}|^2}(\frac{t}{P_{s2}} + \frac{\gamma_{2th}N_{21}}{m_2\rho_d P_{s2}} + \frac{\gamma_{2th}N_{21}}{P_{s2}\rho_d})d_2 t
\end{aligned} \tag{11}$$

where $a_2 = \gamma_{2th}N_{21}N_{22}\rho_2 DT{d_{rd}}^e + \gamma_{2th}\varpi_2 N_{22}N_{21}DT{d_{rd}}^e + \gamma_{2th}N_{22}{\varpi_2}^2 DT{d_{rd}}^e; b_2 = \gamma_{2th}N_{22}\varpi_2 DT{d_{rd}}^e; c_2 = \frac{\gamma_{2th}N_{21}}{\varpi_2} + \frac{\gamma_{2th}N_{21}}{\rho_2} + N_{21}; d_2 = {\varpi_2}^2\eta(1-\rho_2)(D-\varpi_2)T; g_2 = \eta P_{ap2}{\varpi_2}^2$.

The integral is too complicated to solve. We use curve fitting of $e^{-\frac{1}{t+\frac{\rho_d(d_2c_2+g_2)}{d_2}}} => [(0.05254{m_2}^{-0.952} - 0.5023)x^{0.4533{m_2}^{-0.9616}-0.6022}e^{(\frac{-0.04115m_2-0.009699}{m_2+0.1776})x} + 1]$ and $e^{-\frac{1}{\frac{d_2}{(d_2c_2+g_2)\rho_{d_2}}t^2+t}} => [(-0.07916{m_2}^{-0.9075} - 0.3097)x^{0.1469{m_2}^{-0.8948}-1.472}e^{(-0.0199{m_2}^{-0.8146}+0.08933)x} + 0.9998]$ to simplify it.

Finally, the outage probability function can be written as

$$\begin{aligned}
&P_{op2} = 1 + (\rho_2 - 1) * e^{-\frac{\gamma_{2th}N_{21}\rho_2 + \gamma_{2th}N_{21}m_2}{2\theta^2 m_2\rho_2\frac{P_{s2}}{{d_{sr}}^e} + \rho_2 N_{21}}} \\
&- \frac{e^{-\lambda_{12}\frac{\gamma_{2th}N_{22}m_2 DT{d_{rd}}^e}{{m_2}^2\eta(1-\rho_2)(D-m_2)T}}}{\frac{P_{s2}}{{d_{sr}}^e}\left(2\theta^2 + |\frac{{d_{sr}}^e N_{21}}{m_2 P_{s2}}|\right)} e^{-\frac{\gamma_{2th}N_{21}\rho_2 + \gamma_{2th}N_{21}m_2}{2\theta^2 m_2\rho_2\frac{P_{s2}}{{d_{sr}}^e} + \rho_2 N_{21}}} \\
&(0.053{m_2}^{-0.95} - 0.5)^{\alpha_3} \times (-0.079{m_2}^{-0.91} - 0.32)^{\alpha_4} \\
&\frac{\Gamma((0.45{m_2}^{-0.96} - 0.6022)\alpha_3 + (0.147{m_2}^{-0.895} - 1.47)\alpha_4 + 1)}{{z_2}^{(0.45{m_2}^{-0.96}-0.6)\alpha_3 + (0.15{m_2}^{-0.9}-1.472)\alpha_4+1}}
\end{aligned} \tag{12}$$

where $a_2 = \gamma_{2th}N_{21}N_{22}\rho_2 DT{d_{rd}}^e + \gamma_{2th}\varpi_2 N_{22}N_{21}DT{d_{rd}}^e + \gamma_{2th}N_{22}{\varpi_2}^2 DT{d_{rd}}^e$; $b_2 = \gamma_{2th}N_{22}\varpi_2 DT{d_{rd}}^e$; $c_2 = \frac{\gamma_{2th}N_{21}}{\varpi_2} + \frac{\gamma_{2th}N_{21}}{\rho_2} + N_{21}$; $d_2 = {\varpi_2}^2\eta(1-\rho_2)(D-\varpi_2)T$; $g_2 = \eta P_{ap2}{\varpi_2}^2$, also $\alpha_3 = \frac{\frac{\rho_2\lambda_{22}(\frac{a_2}{\rho_2}+2b_2c_2)}{d_2} - \frac{\lambda_{22}b_2\rho_2(d_2c_2+g_2)}{d_2^2}}{\alpha_4 = \frac{\lambda_{22}(a_2c_2+b_2c_2^2\rho_2)}{d_2c_2+g_2}}$

and $z2 = [(\frac{0.041m_2+0.0097}{m_2+0.18})\alpha_3 + (0.02{m_2}^{-0.82} - 0.089)\alpha_4 + \frac{m_2 {d_{sr}}^e}{2\theta^2 m_2\rho_2 P_{s2}+\rho_2 N_{21}{d_{sr}}^e}]$.

C. ACPS

The PDF of $|\hat{h_3}|^2$ is $f_{|\hat{h_3}|^2}(x) = \lambda_{31}e^{-\lambda_{31}x}$, and the CDF is $F_{|\hat{h_3}|^2}(x) = 1 - e^{-\lambda_{31}x}$, where $\lambda_{31} = \frac{1}{2\theta^2+|\frac{N_{31}{d_{sr}}^e}{\varpi_3\rho_c P_{s3}}|}$.

Furthermore, the PDF and CDF of $|\hat{g_3}|^2$ are given as $f_{|\hat{g_3}|^2}(x) = \lambda_{32}e^{-\lambda_{32}x}$ and $F_{|\hat{g_3}|^2}(x) = 1 - e^{-\lambda_{32}x}$ with

$$\lambda_{32} = \frac{1}{r3} \tag{13}$$

where $r3 = \frac{4\theta^4}{2\theta^2+\frac{N_{31}{d_{sr}}^e}{\varpi_3\rho_c P_{s3}}} + N_{32}T\lambda_{31}[\frac{1}{\lambda_{31}\eta|1-\rho_c|\varpi_3 T} + \frac{N_{31}\eta\frac{P_{s3}}{{d_{sr}}^e}|1-\rho_c|\varpi_3 T - \frac{P_{s3}}{{d_{sr}}^e}P_{ap3}}{(\eta\frac{P_{s3}}{{d_{sr}}^e}|1-\rho_c|\varpi_3 T)^2}(-e^{\frac{\lambda_{31}\eta\frac{P_{s3}}{{d_{sr}}^e}|1-\rho_c|\varpi_3 T P_{ap3}}{(\eta\frac{P_{s3}}{{d_{sr}}^e}|1-\rho_c|\varpi_3 T)^2}} Ei(-\frac{\lambda_{31}\eta\frac{P_{s3}}{{d_{sr}}^e}|1-\rho_c|\varpi_3 T P_{ap3}}{(\eta\frac{P_{s3}}{{d_{sr}}^e}|1-\rho_c|\varpi_3 T)^2}))]$.

According to the expressions above, the CDF of γ_{end_3} can be derived from (5) as

$$P_{op3}\{\gamma_{end_3} < \gamma_{3th}\} = F_{\gamma_{end_3}}(\gamma_{3th}) = \int_0^{\frac{\gamma_{3th}N_{31}}{\rho_c m_3 P_{s3}}+\frac{\gamma_{3th}N_{31}}{P_{s3}\rho_c}} f_{|\hat{h_3}|^2}(y)dy + \int_{\frac{\gamma_{3th}N_{31}}{m_3\rho_c^2 P_{s3}}+\frac{\gamma_{3th}N_{31}}{P_{s3}\rho_c}}^{\infty} F_{|\hat{g_3}|^2}[\frac{b_3}{d_3} + \frac{(\frac{a_3}{\rho_c}+2b_3c_3)\frac{d_3}{\rho_c} - \frac{b_3}{\rho_c}(d_3c_3+g_3)}{\frac{d_3^2}{{\rho_c}^2}t + \frac{d_3}{\rho_c}(d_3c_3+g_3)} + \frac{\frac{a_3c_3+b_3c_3^2\rho_c}{d_3c_3+g_3}}{\frac{d_3}{(d_3c_3+g_3)\rho_c}t^2+t}]f_{|\hat{h_3}|^2}(\frac{t}{\rho_c P_{s3}} + \frac{\gamma_{3th}N_{31}}{m_3\rho_c^2 P_{s3}} + \frac{\gamma_{3th}N_{31}}{P_{s3}\rho_c})d_3 t \tag{14}$$

The integral is too complicated to solve. We use curve fitting of $e^{-\frac{1}{t+\frac{\rho_d(d_3c_3+g_3)}{d}}} => [(0.1154{m_3}^{-0.8571} - 0.4076)x^{0.1109{m_1}^{-0.8867}-0.5188}e^{(\frac{-0.04452m_3-0.03081}{m_3+0.6072})x} + 0.9883]$ and $e^{-\frac{1}{\frac{d_3}{(d_3c_3+g_3)\rho_{d_3}}t^2+t}} => [(-0.1138{m_3}^{-0.7688} - 0.4424)x^{0.2295{m_3}^{-0.7929}-1.222}e^{(-0.1211{m_1}^{-0.2713}+1.951)x} + 0.9995]$ to simplify it.

Finally, the outage probability function can be given as

$$P_{op3} = 1-(\rho_c-1)e^{-\frac{\frac{\gamma_{3th}N_{31}}{\rho_c}+\gamma_{3th}N_{31}m_3\rho_c}{2\theta^2 m_3\rho_c\frac{P_{s3}}{{d_{sr}}^e}+|N_{31}|}} - \frac{e^{\frac{-\lambda_{32}\gamma_{3th}N_{32}m_3 DT{d_{rd}}^e}{{m_3}^2\rho_c\eta(1-\rho_c)DT{d_{rd}}^e}}}{\frac{P_{s3}}{{d_{sr}}^e}\left(2\theta^2+|\frac{N_{31}}{m_3\rho_c\frac{P_{s3}}{{d_{sr}}^e}}|\right)}e^{-\frac{\frac{\gamma_{3th}N_{31}}{\rho_c}+\gamma_{3th}N_{31}m_3\rho_c}{2\theta^2 m_3\rho_c\frac{P_{s3}}{{d_{sr}}^e}+|N_{31}|}} (0.12{m_3}^{-0.86}-0.41)^{\alpha_5}(-0.114{m_3}^{-0.77} - 0.44)^{\alpha_6} \frac{\Gamma((0.111{m_1}^{-0.89}-0.52)\alpha_5+(0.23{m_3}^{-0.79}-1.222)\alpha_6+1)}{[z_3]^{(0.112{m_1}^{-0.89}-0.52)\alpha_5+(0.23{m_3}^{-0.79}-1.222)\alpha_6+1}}. \tag{15}$$

where $a_3 = \gamma_{3th}N_{31}N_{32}DT + \gamma_{3th}\varpi_3\rho_3 N_{32}N_{31}DT + \gamma_{3th}N_{32}\rho_3{\varpi_3}^2 DT; b_3 = \gamma_{3th}N_{32}\varpi_3 DT; c_3 = \frac{\gamma_{3th}N_{31}}{\rho_3^2\varpi_3} + \frac{\gamma_{3th}N_{31}}{\rho_3}; d_3 = {\varpi_3}^2\rho_3\eta(1-\rho_3)DT; g_3 = \eta{\varpi_3}^2\rho_3 P_{ap3}$ with $\alpha_5 = \frac{\rho_c\lambda_{32}(\frac{a_3}{\rho_c}+2b_3c_3)}{d_3} - \frac{\lambda_{32}b_3\rho_c(d_3c_3+g_3)}{d_3^2}$, $\alpha_6 = \frac{\lambda_{32}(a_3c_3+b_3c_3^2\rho_c)}{d_3c_3+g_3}$ and $z3 = (\frac{-0.045m_3-0.031}{m_3+0.6072})\alpha_5 + (-0.12{m_1}^{-0.27}+1.95)\alpha_6 - \frac{m_3}{2\theta^2 m_3\rho_c\frac{P_{s3}}{{d_{sr}}^e}+N_{31}}$.

Thus, the achievable rate without a direct link is derived as

$$AR_m = (1 - F_{\gamma_{end_m}}(\gamma_{m_{th}})) \times (\frac{D-\varpi_m}{D}) \tag{16}$$

and the achievable rate with a direct link is derived as

$$AR_{m_d} = [1 - F_{\gamma_{end_m}}(\gamma_{m_{th}})F_{\gamma_{sd}}(\gamma_{m_{th}})] \times (\frac{D-\varpi_m}{D}). \tag{17}$$

V. Numerical results and discussion

In this section, simulation results are discussed. First, we have fixed $P_{s1} = P_{s2} = P_{s3} = 1$; $\eta = 0.5, D = 100, N_{11} = N_{12} = N_{21} = N_{22} = N_{31} = N_{32} = 1$, and defined $\gamma_1 = \frac{|h|^2}{2\sigma^2}$ as the instantaneous SNR of the SR link, and $\gamma_2 = \frac{|g|^2}{2\sigma^2}$ as the instantaneous SNR of the RD link, where $g_1 = g_2 = g_3 = g$, and $h_1 = h_2 = h_3 = h$. Based on [3], the ambient RFEH is defined as $P_{ARF} = S_{ba} \times A_{real}, A_{real} \approx G(f_0)\frac{{\lambda_0}^2}{4\pi}$, where S_{ba} is the banded input RF power density in W/cm^2, that is calculated by summing all the spectral peaks across the band, A_{real} is the real aperture (or capture area) of the antenna, λ_0 is the free-space wavelength at the midband frequency f_0 and $G(f_0)$ is the rectenna's antenna gain at f_0.

From [3], by using the GSM1800 Tape protocol, the maximum power achieved is $\mathrm{W/cm^2}$ and the maximum power density is approximately $450\ \mathrm{nW/cm^2}$. Therefore, we assume the out-of-band ambient RF energy harvested at the relay node is constant, $P_{ap1} = P_{ap2} = P_{ap3}$, and has a value of 0.0003 [3].

A. Achievable Rate Evaluation

Fig. 3, Fig. 4 and Fig. 5 display the relationships between the achievable rates and the power splitting ratios when γ_1 and γ_2 are both fixed at 10 dB. For ACEPS in Fig. 3, the AR first increases and then decreases when ϖ_1 or ρ_1 increases. In this case, it can be observed that the optimal values are $\varpi_1 = 15$ and $\rho_1 = 0.3$, and the maximum AR is around 0.545.

For ADTPS in Fig. 4, it can be observed that the AR first increases and then decreases when ϖ_2 increases. Moreover, the AR always monotonically decreases when ρ_2 increases. Thus, in this case, the only optimal value is $\varpi_2 = 40$, and the maximum AR is around 0.72. Thus, the performance of the ADTPS structure can only be optimised through by the number of pilots.

For ACPS in Fig. 5, we compared the simulation result with the analytical result and we can see they match with each other very well, which has proved the validity of the scheme. Also it can be seen that the AR first decreases and then increases when ρ_3 increases. In this case, it can be observed that the optimal value is $\rho_3 = 0.8$, and the maximum AR is around 0.5.

From these results, it can be recognised that the ACPS structure has the largest achievable rate, and thus the best performance among the three proposed structures. It assigns more power the pilots to improve channel estimation, at the

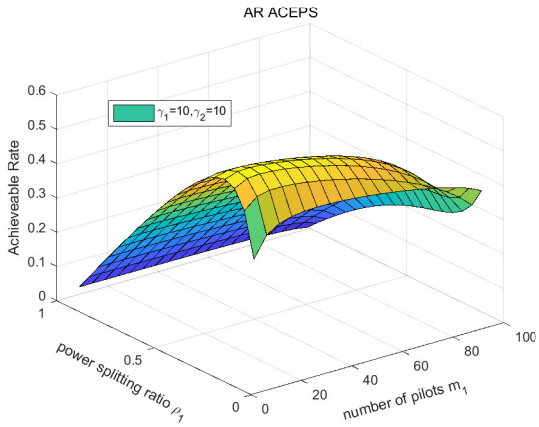

Fig. 3. Achievable rate of ACEPS with a direct link, versus the power splitting ratio ρ_1 and number of pilots m_1, when γ_1 and γ_2 are fixed at 10 dB and 10 dB.

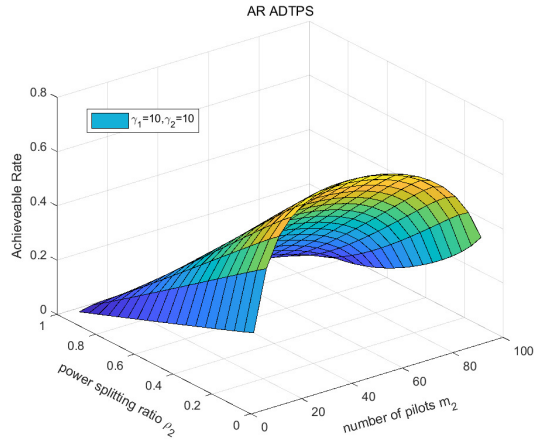

Fig. 4. Achievable rate of ADTPS with a direct link, versus the power splitting ratio ρ_2 and number of pilots m_2, when γ_1 and γ_2 are fixed at 10 dB and 10 dB.

expense of less harvested energy. When comparing Fig. 3, Fig. 4 and Fig. 5 with the results in [12] under the same conditions, the hybrid structures have a significant improvement.

VI. Conclusions

In this letter, three improved hybrid SWIPT/ambient EH structures have been investigated. Numerical results have verified the optimal values for the different structures. When the data packet size is constant, the hybrid EH schemes have a better performance than using the energy from the source only ACPS has the best capabilities.

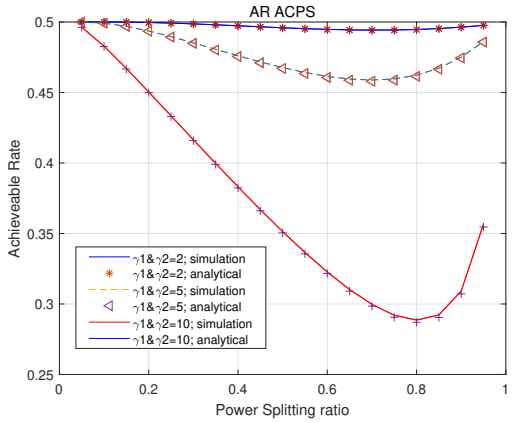

Fig. 5. Numerical and Computational Achievable rate results of ACPS with a direct link, versus the power splitting ratio ρ_3, when γ_1 and γ_2 are both fixed at 2 dB, 5dB and 10 dB, respectively.

References

[1] X. Lu, P. Wang, D. Niyato, D. I. Kim, and Z. Han, "Wireless networks with rf energy harvesting: A contemporary survey," *IEEE Communications Surveys and Tutorials*, vol. 17, no. 2, pp. 757–789, 2015.

[2] Y. Chen, "Energy-harvesting af relaying in the presence of interference and nakagami-m fading," *IEEE Transactions on Wireless Communications*, vol. 15, no. 2, pp. 1008–1017, 2016.

[3] M. Piñuela, P. D. Mitcheson, and S. Lucyszyn, "Ambient rf energy harvesting in urban and semi-urban environments," *IEEE Transactions on microwave theory and techniques*, vol. 61, no. 7, pp. 2715–2726, 2013.

[4] F. Yildiz, "Potential ambient energy-harvesting sources and techniques." *Journal of technology Studies*, vol. 35, no. 1, pp. 40–48, 2009.

[5] R. J. Vyas, B. B. Cook, Y. Kawahara, and M. M. Tentzeris, "E-wehp: A batteryless embedded sensor-platform wirelessly powered from ambient digital-tv signals," *IEEE Transactions on microwave theory and techniques*, vol. 61, no. 6, pp. 2491–2505, 2013.

[6] V. Marian, B. Allard, C. Vollaire, and J. Verdier, "Strategy for microwave energy harvesting from ambient field or a feeding source," *IEEE Transactions on Power Electronics*, vol. 27, no. 11, pp. 4481–4491, 2012.

[7] Y. Chen, W. Feng, R. Shi, and N. Ge, "Pilot-based channel estimation for af relaying using energy harvesting," *IEEE Transactions on Vehicular Technology*, vol. 66, no. 8, pp. 6877–6886, 2017.

[8] S. Shen, Y. Zhang, C. Y. Chiu, and R. Murch, "Directional multiport ambient rf energy harvesting system for the internet of things," *IEEE Internet of Things Journal*, pp. 1–1, 2020.

[9] H. Cheng, C. Wang, and X. Zhang, "An opportunistic routing in energy-harvesting wireless sensor networks with dynamic transmission power," *IEEE Access*, vol. 7, pp. 180 652–180 660, 2019.

[10] H. Zhang, J. Du, J. Cheng, K. Long, and V. C. M. Leung, "Incomplete csi based resource optimization in swipt enabled heterogeneous networks: A non-cooperative game theoretic approach," *IEEE Transactions on Wireless Communications*, vol. 17, no. 3, pp. 1882–1892, 2018.

[11] Y. Liang, B. Li, R. Zhang, H. Li, and S. Zhao, "Distributed beamforming for energy-harvesting relaying in vehicular networks," *Journal of Communications and Information Networks*, vol. 5, no. 2, pp. 160–167, 2020.

[12] Y. Zhou and Y. Chen, "Novel energy-harvesting af relaying schemes with channel estimation errors," *IEEE Systems Journal*, vol. 14, no. 1, pp. 333–342, 2020.